Waveguide Arc Study

H. C. Yen
Radio Frequency and Microwave Subsystems Section

This is the second article in the series reporting the progress of waveguide arc study undertaken by the Transmitter Group. In this article we report some experiments and their preliminary results on the arc study and the arc detector evaluation. Some future experiments are also briefly discussed.

I. Introduction

This is the second article in the series reporting the progress of waveguide arc study and protection undertaken by the Transmitter Group. In this article we briefly describe some experiments that have been or are being carried out to investigate the arc properties and to evaluate the arc detection subsystem performance. Preliminary results are presented where appropriate.

II. Controlled RF Arc Generation

Our arc study will be based on a controlled RF arc established in the laboratory; therefore, a method of generating a suitable arc has to be found. At present, we are experimenting with the idea of establishing an arc inside a resonant structure. During this phase of study, a matched waveguide system with a resonant section was assembled. A block diagram showing the essential components and the signal path is given in Fig. 1. The RF power amplifier used here is capable of delivering more than 10 W into a matched load. The resonant section is made of a 10.16-cm-long standard waveguide (WR430) with both ends enclosed with conducting planes. The coupling is achieved through iris openings in these conducting planes. The width for the input plane is such that, along with the stub tuner, zero-reflected RF power can be achieved at resonance. The iris width on the output plane is such that the loading on the resonator is negligible while providing a measurable signal for monitoring the RF fields inside the resonator.

Preliminary results showed that the unloaded quality factor of the resonator can be as high as 6.5×10^3 at 2 GHz. Since the RF source used in this experiment was not stabilized, the critical coupling state (zero reflection power at resonance) could not be maintained for long before detuning occurs due to oscillator drift and/or thermal effects. At present, we are exploring other alternatives. Among them, the scheme of using a very stable VHF oscillator in cascade with a frequency multiplier seems very promising in providing the necessary stable RF drive.

The idea of using a resonant structure is to sustain a very high RF field inside the structure with a low-power RF source. However, as soon as a breakdown is induced, the loading on the resonator can be such that a large mismatch between the source and the resonator occurs, resulting in substantially reduced fields inside. This, in turn, can quench the arcing unless the already formed arc can be sustained at a much lower field level. (This is in contrast to the arcs generated in a

high-power transmission system where arcs are continuously subject to intense incident RF until the latter is turned off.) Such difficulty is inherent in any experiment using a resonator to study the properties of a not-negligible perturbation introduced to it. Nevertheless, arc study using a resonant structure still merits further pursuit for the following reasons. During the initial breakdown of high-power transmission, arcs evolve from a rapid formative (initiation) state into a more prolonged sustained state. The field and energy balance conditions to bring about an RF arc and to sustain it are believed to be quite different, as is the case for the dc arcs. In view of protecting the transmitter, it is logical and desirable to design an arc detector to be most responsive to the waveguide arc characteristics that are exhibited during the formative stage of arcing, in addition to being responsive to the emission from an established arc. The short-lived (but readily repetitive) pulsed arcs permitted by the resonator are useful in studying the nature of this formation phase of arcing because the RF fields inside the resonator prior to the breakdown can be made to approach that present in the waveguide of a high-power transmission system, and therefore resonator arcs are expected to be good simulations of high-power waveguide arcs as far as this phase is concerned.

Since the arc formation time was reported to be quite short (about 1 microsecond at 5 kW, and much less at higher power), a prudent design requires that the arc detector should also respond positively during the following sustained state. Thus some knowledge about the sustained arcs whether they are moving (such as those that exist further along the transmitter output waveguide) or stationary (such as those that may exist at the klystron window) is also highly desirable. Methods of generating sustained RF arcs inside a resonator are currently being explored so that studies can be done using them as a source. Such arcs are not expected to be fully commensurate with existing high-power transmitter arcs; nevertheless, at this early stage of the detector engineering design, we do not wish to tie up a multimillion dollar, megawatt facility to test arc detector responsitivity. Of course, high power RF arcs are eventually needed for final verification tests.

III. DC Nitrogen Arc Experiment

During this phase of study, we also performed some dc nitrogen arc experiments mainly as an exercise of getting acquainted with the optical instrument as well as the flickering nature and radiation spectrum of nitrogen arcs. A block diagram showing the basic experimental arrangement is given in Fig. 2.

The optical instrument consists entirely of an EG&G 580/585 Spectroradiometer system. It has the capability of performing both spectrometer and radiometer measurements, but is calibrated for only the former mode of operation. When measuring the spectral distribution of a source, order sorting filters are needed for each segment of the spectrum with bandwidth 100 ~ 200 nm wide to eliminate the higher-order contributions from shorter wavelengths for a given grating position. The overall spectral range is determined by the filter type used, grating range, and photomultiplier responsivity. For our system, it covers from 350 to 1200 nm with two different photomultiplier detectors. The accuracy of the wavelength reading is estimated to be ±5 nm mainly due to a mechanical backlash in the grating scanning mechanism.

The arc was generated across a 3.2-mm gap between two tungsten electrodes with voltage of 10 to 15 kV across them. The tube was repeatedly evacuated and refilled with 1 atmosphere of dry nitrogen gas. The maximum arc current is limited by the high-voltage supply to 1 mA and as a result only a very limited light output has been obtained.

A typical raw spectrum covering the visible range is shown in Fig. 3. The spectrum is somewhat distorted because the spectrometer has quite different responsitivities over different portions of the spectral regions. After correcting for this difference, a "true" spectrum is obtained. This is a very time consuming process because it has to be done for each wavelength. Compounding the task are the original uncertainty of the raw spectrum and the possible errors in wavelength designation. In Fig. 3 we also show a sample of a corrected spectrum. As can be seen from there, detail spectral structures cannot be unambiguously resolved because of spectrometer resolution, spectrum fluctuation, wavelength errors, and the correction process for responsitivity difference. Nevertheless, such spectrum can still provide a general sketch of spectral distribution and their relative magnitude.

For wavelengths between 700 and 1200 nm, a thermoelectrically cooled infrared detector has to be used. At present we have some difficulties obtaining a consistent spectrum in this region largely due to the drift and dark current in the detector itself. This seems to imply insufficient cooling power for our detector. Further study of this problem is under way.

One useful parameter to describe the general characteristics of an arc is the arc temperature, especially when local thermodynamic equilibrium prevails. An empirical method has been established (Ref. 1) that can determine this temperature very conveniently. Specifically, for a given pressure, the nitrogen arc radiation (per unit source volume, per unit wavelength bandwidth and per unit solid angle) at wavelength $\lambda = 4955\text{Å}$ is measured. The arc temperature is then read off from an experimentally established calibration curve showing the same quantity as a function of temperature. This particular

wavelength is chosen because, in the vicinity of it, there is no line spectrum contribution (i.e., pure continuum) even at a very elevated temperature. Whereas in other parts of the spectrum, substantial contribution from line spectrum broadening can take place at elevated temperatures even though they are also devoid of line spectrum contribution at a lower temperature. Applying this scheme to our sample spectrum, the temperature was found to be well below 3000 K, which is consistent with the fact that the arc current is limited to less than 1 mA. To our knowledge, there is no nitrogen spectrum at this temperature, pressure, and arc current readily available for comparison; therefore, to establish confidence in our measurement technique, spectra at much higher arc currents are needed.

IV. Transmitter Test Light Upgrading

A nitrogen atmosphere test light would be quite desirable as a light source for arc detector testing. However, until such a unit can be developed and implemented, the xenon-type flash lamp seems to be an interim cost effective test lamp despite the fact that the spectrum it produces is different. In fact, such a lamp can perform almost all the functions that we expect from an ideal nitrogen test light.

A feasibility study of upgrading the existing transmitter test light subsystem was initiated during this phase of study. The goal of this study is to evaluate a commercial solid state electronic camera flash as a candidate for replacing the presently used test light. The attractive features of the flash unit used in this study (Kodak Ektra Electronic Flash) are small size, low-voltage power source (3 V), fast rise time, and intense light output.

The test light is mounted on the transition region from the klystron amplifier output window to a WR430 elbow section. It performs routine arc detector checks, provides a time reference for response time check and can be used in the arc detector sensitivity calibration, which in turn provides the necessary information for setting the detector safety margin.

The unit was slightly modified so that it could be electronically triggered to provide well-controlled and repetitive unambiguous flashings. At the recommended +3 V supply, it required three or four seconds to fully charge the unit with peak charging current as high as 1.5 A. The standard arc detector was used to detect the flash via an optical fiber link at the bend of the elbow. The time delay from the rising edge of the triggering pulse to the rising edge of the arc detector output was measured at several test light levels. The results are summarized in Fig. 4.

Ith is the threshold intensity to produce an observable detector output. Since both pulses have rather short rise times (of the order of nanoseconds), the observed delay can be attributed to the combination of the delay in actual flashing, delay due to light path, delay due to photodiode response, and delay due to voltage comparator (LM211) in the arc detector circuitry. On the time scale of observed delay, it seems that most of the delay is due to the voltage comparator response when the input voltage to it is small (i.e., at very low-light level). This is partially supported from the specification of said comparator where it is shown that substantial response time is required at low input level. To show the weakening effect on the light eventually detected by the photodiode due to the waveguide and optical fiber link, the "dead" time of the system was measured by directly connecting the flash unit output port to the arc detector input port. At maximum flash output, the delay time was measured at 0.7 μs as opposed to the minimal observed time of 6 μs in the actual waveguide configuration.

Clearly, from the results obtained, we conclude, to make an arc detector effective and reliable, every step of caution has to be taken to assure the maximum amount of light reaching the photodiode surface. Assuming that the detector remains unaltered, the following areas for improvement remain: waveguide wall reflectivity, optical acceptance geometry, optical fiber attenuation, and optical fiber-to-photodiode coupling. Among them, the acceptance geometry and fiber-diode coupling seem to offer more room for improvement. Only the coupling problem will be discussed here and we will say more about optical acceptance geometry in the next section.

On a closer examination of our hardware, we found that the optical fiber-to-photodiode coupling was rather poor in our present set up. The problem arises mainly from the physical construction of the fiber itself, which is custom-made and has two input and two output channels. The individual tiny fibers that constitute the main optical fiber are so arranged that whenever there is light in either input channel, it will be equally split into two output channels. Ideally we would like to have the light emerging from the output channel uniformly distributed over the whole cross-section area to maximize the effective interception between this cross section and the photodiode active surface because they are not of the same size and shape. Unfortunately, this is not the case for our fibers. The light emerging from our optical fiber tends to cluster in patches and is distributed irregularly over the cross section. With the active photodiode surface smaller than the optical fiber cross section, the effective light coupling can be severely reduced depending on the actual light distribution.

An attenuation experiment was carried out to investigate the loss due to this "optical mismatch." A monochromatic light source, whose size is the same as the diameter of an

optical probe aperture used for detecting the light at the output end but less than that of the optical fiber, provides a uniform illumination on the input cross section. The results of the measurement were summarized in Table 1. Judging from the state of the art of optical fiber technology and taking into account the length involved and the power splitting feature, an attenuation of 5.0 ~ 5.5 dB between channels is regarded as normal. We have incurred an additional attenuation of up to 3.1 dB due to poor coupling. This deficiency in coupling can be corrected without difficulty. If we exchange the roles of input and output channels, we can obtain a uniform light output over the entire cross section at the input channels.

V. LED Array Simulation Experiment

One piece of design information that is useful in maximizing the amount of light received by the detector is the fraction of the light output that enters the optical fiber for a given source and fiber configuration. Not knowing where the breakdown will occur in the general area of the klystron amplifier output window, it is impossible to obtain a specific answer. In the following, we attempt to make an order-of-magnitude estimate of this fraction based on the assumption that the arc will strike across the center of the broad wall of the waveguide at the far end where the test light is situated. A linear LED array was used to simulate the arc. Its dimension is 3.2 mm × 50.8 mm, and at a distance of more than 50 cm away, it can be regarded as an effective point source. The desired fraction is then obtained by taking the ratio of the amount of light received at the input end of the optical fiber to the light intensity of the source. The optical measurement is similar to that shown in Fig. 2 and the essential data are summarized below:

P = Total light emitted from the source per unit solid angle per unit wavelength (i.e., irradiant intensity per unit wavelength)

$= 2.14 \times 10^{-6}$ W/nm-rad

I_r = Total light received at the input end of the optical fiber per unit wavelength

$= 4.1 \times 10^{-10}$W/nm

Therefore the effective solid angle subtended is

$$\Omega_{eff} = \frac{I_r}{P} = 1.9 \times 10^{-4} \text{ rad}$$

However, the apparent solid angle is approximately

$$\Omega_{app} \approx 9.0 \times 10^{-5} \text{ rad}$$

That is, the effective solid angle is twice the apparent solid angle indicating that the contribution of light indirectly scattered into the optical fiber is not insignificant. In fact, it is quite comparable to that from direct scattering. One other aspect worthy of note from the above calculation is that a linear source can radiate into a solid angle of the order of π radians while our effective solid angle is only about 2×10^{-4} radian, i.e., only about 0.01 percent of the light gets detected in our present geometry. It seems reasonable to assume this collection efficiency can be improved somewhat by enlarging the aperture of the optical fiber until the electromagnetic characteristics of the system start to be affected.

Reference

1. J. C. Morris, R. U. Krey and G. R. Bach, "The Continuum Radiation of Oxygen and Nitrogen for Use in Plasma Temperature Determination," *J. Quant. Spectrosc. Radiat. Transfer*, Vol. 6, pp. 727-740.

Table 1. Optical fiber attenuation and one of the test configurations

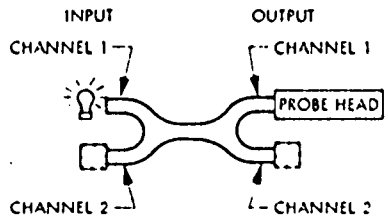

Input channel	Output channel	Attenuation, dB ± 0.3
1	1	6.2
1	2	8.6
2	1	7.6
2	2	6.1

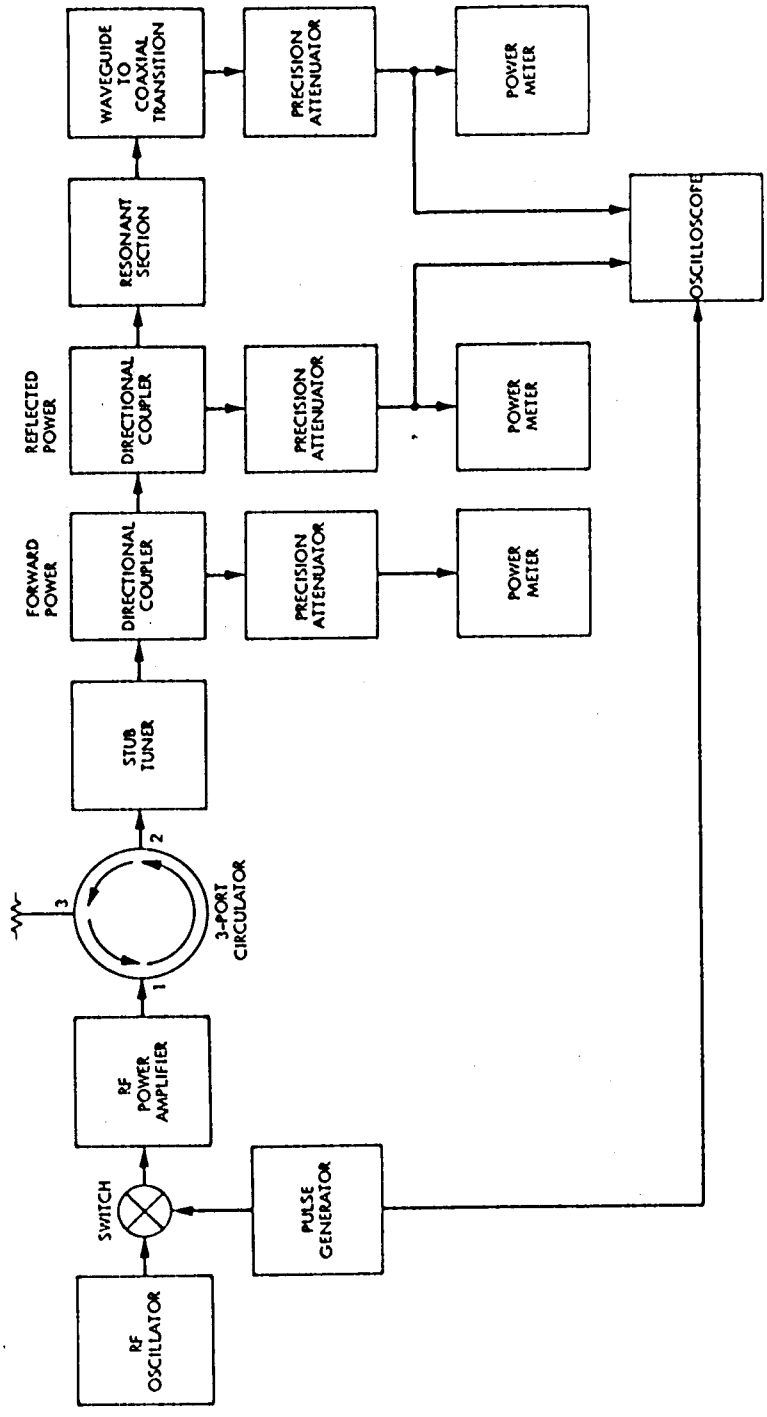

Fig. 1. Block diagram showing the signal path for the experiment of controlled RF arcs

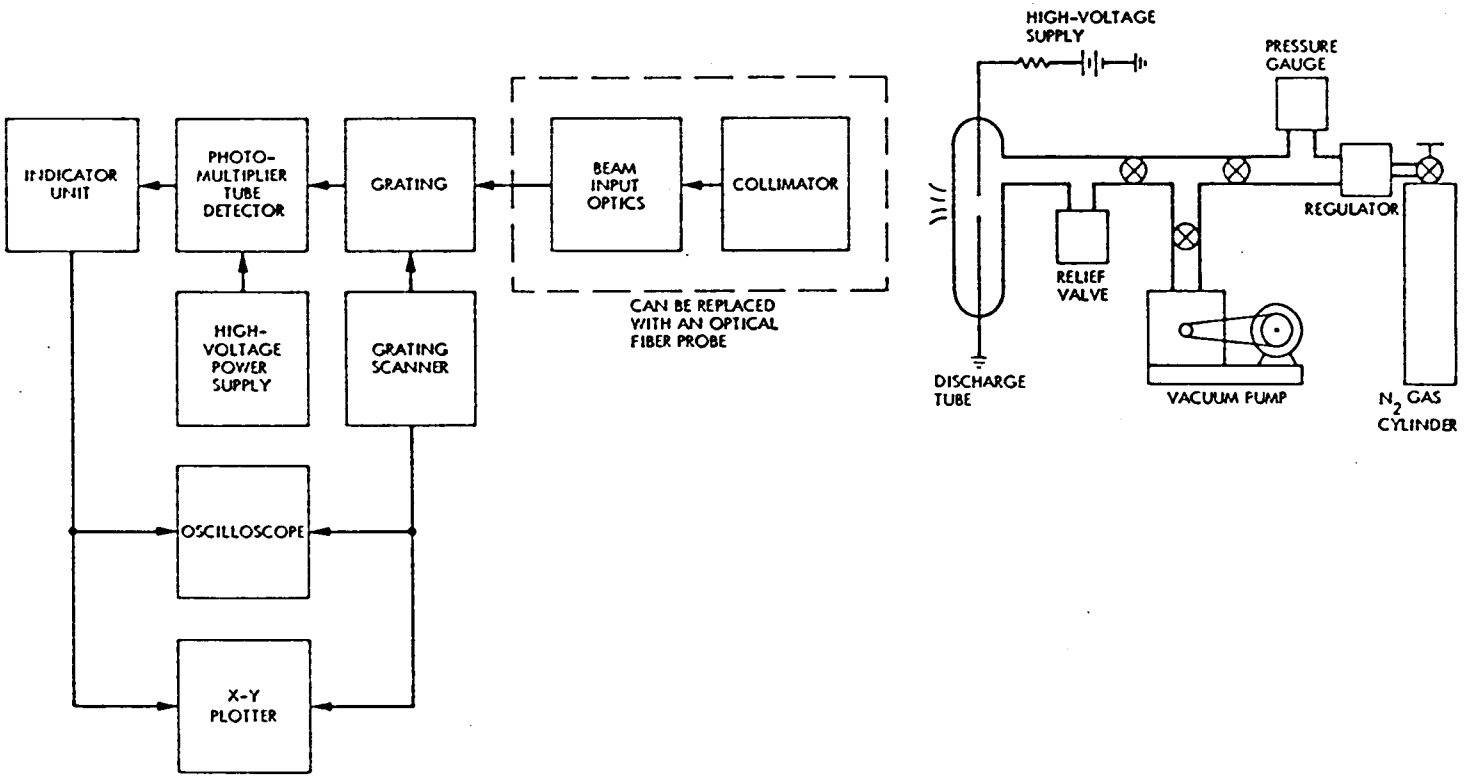

Fig. 2. Experimental set up for dc nitrogen arc study

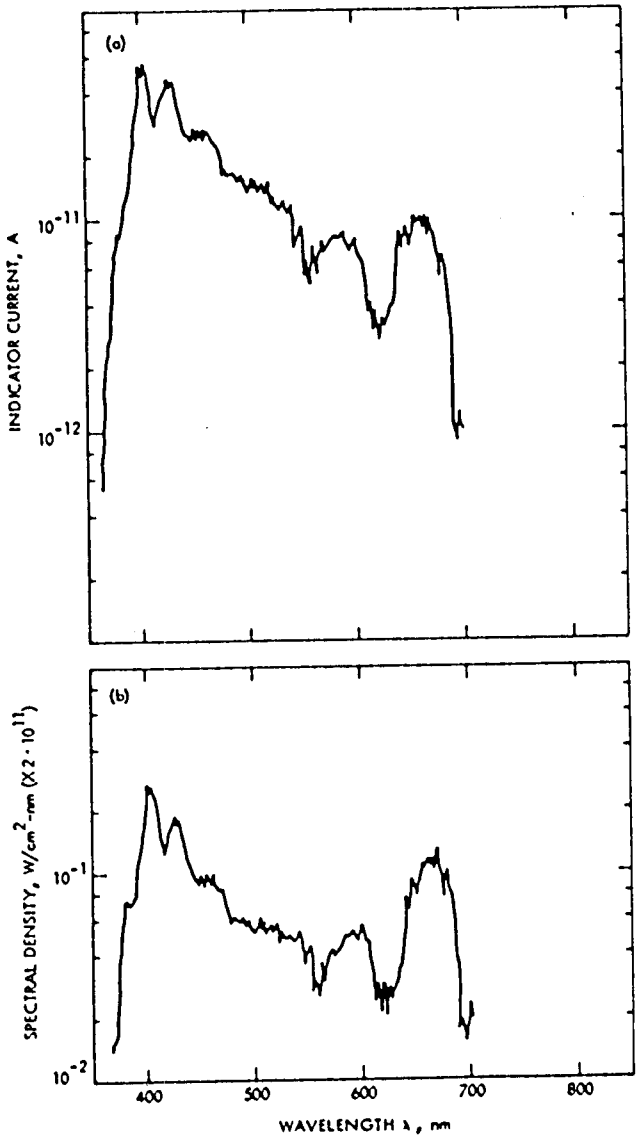

Fig. 3. Nitrogen spectrum: (a) a sample of raw spectrum; (b) the same spectrum after correction

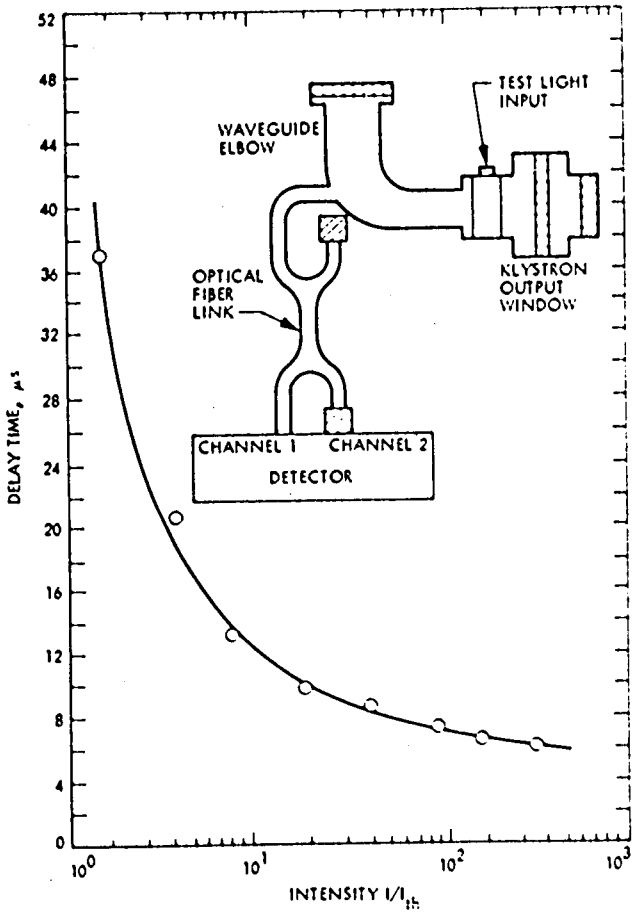

Fig. 4. Delay time versus test light intensity